

# Instabilities in Biaxially Loaded Rectangular Membranes and Spherical Balloons Made of Compressible Isotropic Hyperelastic Materials

R. C. BATRA

*Department of Engineering Science and Mechanics, M/C 0219, Virginia Polytechnic Institute and State University, Blacksburg, VA 24061, USA*

(Received 15 January 2003; accepted 13 May 2003)

*Dedication to Professor M. Hayes for his pioneering work in Mechanics.*

**Abstract:** We analyze homogeneous deformations of a rectangular rubberlike membrane loaded by equal normal tensile dead loads on the edges, and of a spherical rubber balloon inflated by a constant pressure. The rubber is modeled as an isotropic compressible hyperelastic material. Three material models, namely the harmonic, the generalized Blatz–Ko, and the St Venant–Kirchhoff models, are employed. It is found that Treloar’s instability, i.e. the occurrence of unequal principal stretches in a square membrane under equal normal dead loads, is not admissible in the harmonic and the St Venant–Kirchhoff materials, but is admissible in some Blatz–Ko materials. For each one of the three materials, the pressure–radius relation for the inflation of a spherical balloon does not exhibit the non-monotonicity seen for a Mooney–Rivlin material.

**Key Words:** Treloar’s instability, nonlinear elasticity, stored energy function, analytical solution

## 1. INTRODUCTION

Two frequently studied instabilities in non-linear elasticity are the asymmetric principal stretches in a homogeneous isotropic square membrane under equal biaxial tensile dead loads [1–5], and the non-monotonic pressure–radius relation during the inflation of a spherical balloon [2, 4, 6]. In each case the deformation is homogeneous. Bifurcations of the homogeneously deformed spherical balloons into inhomogeneously deformed nonspherical shapes have been analyzed by Chen and Healey [7] and Haughton [8]. Carroll [9] has given a simple condition on the material response curve for uniaxial compression to classify incompressible hyperelastic materials into three classes for analyzing their behavior regarding the inflation of a spherical balloon. The pressure may increase monotonically, or it may increase and then decrease, or it may increase, decrease and then increase again. Haughton [8] has investigated the inflation of a spherical balloon made of a compressible hyperelastic material, and the bifurcation of the spherical shape into nonspherical ones. He showed that, for a compressible Ogden [10] material, bifurcation points strongly depend upon the dilatation. Haughton [8] did not impose the requirement that the transverse stretch of the balloon thickness must be positive.

We note that Rivlin [11] found seven equilibrium configurations of a cube made of a homogeneous neo-Hookean material. He showed that of the seven, only one, the undeformed configuration, has all the symmetries of the given loading and is unstable for sufficiently large values of tensile loads. However, asymmetric homogeneous deformations do not occur under equal biaxial dead loads in a homogeneous and isotropic square membrane made of a neo-Hookean material but are possible in a Mooney–Rivlin material. Previous analyses [1–5] of deformations of the membrane have assumed that the material is incompressible. Here we investigate if asymmetric deformations in a square membrane under equal biaxial dead loads and the non-monotonic pressure–radius relation for a spherical balloon also occur in a compressible hyperelastic material. We consider three constitutive relations, namely the harmonic material proposed by John [12, 13], the Blatz–Ko material [14, 15] and the St Venant–Kirchhoff material [16]. These materials are characterized by the shear modulus and the Poisson ratio defined for infinitesimal deformations; the constitutive relation for the Blatz–Ko material also has an additional non-dimensional parameter with values between 0 and 1. Treloar [17] observed unequal principal stretches during homogeneous deformations of a square membrane subjected to equal normal dead loads on the edges; Ericksen [2] called this phenomenon Treloar’s instability.

Batra [18] has analyzed biaxial homogeneous deformations of a homogeneous rectangular elastic membrane with four objective constitutive relations linear in suitable measures of stress and strain. Of these, three constitutive relations including the St Venant–Kirchhoff material admitted the possibility of Treloar’s instability. However, the stability of the symmetric and the asymmetric solutions was not investigated primarily because three of these materials were not hyperelastic. One could have determined the stability of the deformed configuration by analyzing the growth of infinitesimal deformations superimposed upon a finitely deformed body.

## 2. PRELIMINARIES

We assume that the body is made of a homogeneous, isotropic and unconstrained elastic material. The class of homogeneous deformations studied is such that with respect to either a local or a global orthonormal set of basis functions the deformation gradient is a constant diagonal matrix, namely

$$\mathbf{F} = \begin{bmatrix} \lambda_1 & 0 & 0 \\ 0 & \lambda_2 & 0 \\ 0 & 0 & \lambda_3 \end{bmatrix}. \quad (2.1)$$

$\lambda_1$ ,  $\lambda_2$  and  $\lambda_3$  are principal stretches along the  $x_1$ ,  $x_2$ , and  $x_3$  coordinate axes respectively. Thus in the polar decomposition  $\mathbf{F} = \mathbf{R}\mathbf{U} = \mathbf{V}\mathbf{R}$  of  $\mathbf{F}$ ,  $\mathbf{R}$  is the identity matrix, and  $\mathbf{U} = \mathbf{V} = \mathbf{F}$ . The principal invariants  $I_B$ ,  $II_B$  and  $III_B$  of the left Cauchy–Green tensor  $\mathbf{B} = \mathbf{F}\mathbf{F}^T$  are given by

$$I_B = \lambda_1^2 + \lambda_2^2 + \lambda_3^2, \quad II_B = \lambda_1^2 \lambda_2^2 + \lambda_2^2 \lambda_3^2 + \lambda_3^2 \lambda_1^2, \quad III_B = \lambda_1^2 \lambda_2^2 \lambda_3^2. \quad (2.2)$$

For an isotropic compressible hyperelastic material, the strain energy density  $W$  per unit reference volume is a function of the three principal invariants of  $\mathbf{B}$ . The first Piola–Kirchhoff stress tensor  $\mathbf{T}$  and the Cauchy stress tensor  $\boldsymbol{\sigma}$  can be derived from  $W$  through [16]

$$\mathbf{T} = \frac{\partial W}{\partial \mathbf{F}}, \quad \boldsymbol{\sigma} = \frac{1}{J} \mathbf{T} \mathbf{F}^T, \quad J = \det \mathbf{F}. \quad (2.3)$$

Alternatively,  $W$  can be expressed as a symmetric function of the three principal stretches  $\lambda_1$ ,  $\lambda_2$  and  $\lambda_3$ . The three principal stresses  $T_{11}$ ,  $T_{22}$  and  $T_{33}$  are given by

$$T_{\alpha\alpha} = \frac{\partial W}{\partial \lambda_\alpha}, \quad \alpha = 1, 2, 3, \text{ no sum on } \alpha. \quad (2.4)$$

The functional forms of the strain energy density,  $W$ , for the three materials studied are given below.

#### *a. Harmonic Material*

The strain energy density for a harmonic material, proposed by John [12, 13], was motivated by mathematical convenience rather than by experimental evidence. This material has been studied earlier by Ogden and Isherwood [19], Abeyaratne and Horgan [20], and Jafari et al. [21]; its properties are quite different from those of the other two materials investigated here. The functional form of  $W$  is

$$W = 2\mu_0[H(I_U) - III_U + 1], \quad (2.5)$$

where  $\mu_0$  is the shear modulus for infinitesimal deformations, and the scalar function  $H$  satisfies certain inequalities [22]. We use the following expression for  $H$  proposed by Haughton and Lindsay [23]:

$$H(I_U) = I_U - 3 + \alpha(I_U - 3)^2, \quad \alpha = \frac{1 - \nu_0}{2(1 - 2\nu_0)}, \quad (2.6)$$

where  $\nu_0 \neq 1/2$  is the Poisson ratio for infinitesimal deformations. Substitution from (2.5) and (2.6) into (2.3) gives

$$\boldsymbol{\sigma} = 2\mu_0 \mathbf{R} \left[ -\mathbf{1} + \frac{1 + 2\alpha(I_U - 3)}{III_U} \mathbf{U} \right] \mathbf{R}^T, \quad (2.7)$$

where  $\mathbf{1}$  is the identity matrix.

#### *b. Generalized Blatz–Ko Material*

For the generalized Blatz–Ko material [14]

$$\begin{aligned} W = & \frac{\mu_0 f}{2} \left[ (I_B - 3) - \frac{2}{q} (III_B^{q/2} - 1) \right] \\ & + \frac{\mu_0(1-f)}{2} \left[ \left( \frac{II_B}{III_B} - 3 \right) - \frac{2}{q} (III_B^{-q/2} - 1) \right], \end{aligned} \quad (2.8)$$

where

$$q = -\frac{2\nu_0}{1 - 2\nu_0}, \quad (2.9)$$

and  $f$  is a material parameter between 0 and 1.  $f = 0$  describes a class of foamed polyurethane elastomers and  $f = 1$  characterizes a class of solid polyurethane rubbers studied in the Blatz–Ko experiments [14]. Equation (2.8) can also be derived theoretically; e.g., see Beatty [15]. For  $\nu_0 = 1/4$ , Equation (2.8) does not satisfy the empirical inequalities [16]. From (2.8) and (2.3) we get

$$\boldsymbol{\sigma} = \mu_0 \left[ \left( -f III_B^{(q-1)/2} + (1-f) III_B^{-(q-1)/2} \right) \mathbf{1} + \frac{f}{III_B^{1/2}} \mathbf{B} - \frac{1-f}{III_B^{1/2}} \mathbf{B}^{-1} \right]. \quad (2.10)$$

*c. St Venant–Kirchhoff Material*

For this material [16]

$$W = \frac{1}{2} (\lambda_0 + 2\mu_0) I_E^2 - 2\mu_0 II_E, \quad (2.11)$$

has the same form as in the linear elasticity theory with the strain tensor for the infinitesimal deformations that is linear in displacement gradients replaced by the Green–St Venant strain tensor  $\mathbf{E} = (\mathbf{C} - \mathbf{1})/2$ ,  $\mathbf{C} = \mathbf{F}^T \mathbf{F}$ . Note that  $\mathbf{E}$  also has quadratic terms in displacement gradients.  $\lambda_0$  and  $\mu_0$  in (2.11) are the Lamé constants. Equations (2.3) and (2.11) give

$$\boldsymbol{\sigma} = \frac{\mu_0}{\sqrt{III_B}} \left[ -II_B \mathbf{1} + \left( I_B - 1 - \frac{q}{2} (I_B - 3) \right) \mathbf{B} + III_B \mathbf{B}^{-1} \right]. \quad (2.12)$$

The two problems studied herein are now described.

*(i) Biaxial stretching of a rectangular membrane*

With the  $x_1$  and  $x_2$  axes of a rectangular Cartesian coordinate system aligned along the edges of a rectangular membrane, it is assumed that the deformation gradient (2.1) describes homogeneous deformations of the membrane under the action of equal and oppositely directed dead surface tractions  $\bar{T}_{11}$  and  $\bar{T}_{22}$  at the edge surfaces  $X_1 = 0, a$  and  $X_2 = 0, b$ .  $\mathbf{X}$  denotes the place occupied by a material particle in the unstressed reference configuration that in the current configuration is at  $\mathbf{x}$ . Treloar's [17] test data supports our assumption of the form (2.1) of the deformation gradient  $\mathbf{F}$ . We note that for an incompressible isotropic elastic membrane, Chen [3] has analyzed the stability of the deformed configuration of the membrane under all homogeneous deformations. The stretch  $\lambda_3$  in the transverse direction as a function of the in-plane stretches  $\lambda_1$  and  $\lambda_2$  is determined from the condition

$$T_{33} = \frac{\partial W}{\partial \lambda_3} = 0 \text{ or } \sigma_{33} = 0, \quad (2.13)$$

which holds because the top and the bottom surfaces of the membrane are traction free and we are studying its homogeneous deformations. Substitution for  $\lambda_3$  in terms of  $\lambda_1$  and  $\lambda_2$  in the strain energy density function gives

$$\tilde{W} = \tilde{W}(\lambda_1, \lambda_2) = W(\lambda_1, \lambda_2, \lambda_3(\lambda_1, \lambda_2)). \quad (2.14)$$

For an isotropic material  $W$  is a symmetric function of  $\lambda_1$ ,  $\lambda_2$  and  $\lambda_3$ , and  $\tilde{W}$  is a symmetric function of  $\lambda_1$  and  $\lambda_2$ . Stable equilibrium configurations of the membrane are described by the absolute or the relative minima of the thermodynamic potential [2] or the free enthalpy [4]

$$E(\lambda_1, \lambda_2) = \tilde{W}(\lambda_1, \lambda_2) - \bar{T}_{11} \lambda_1 - \bar{T}_{22} \lambda_2 \quad (2.15)$$

for fixed values of  $\bar{T}_{11}$  and  $\bar{T}_{22}$ . Thus, in an equilibrium configuration

$$\bar{T}_{11} = \frac{\partial \tilde{W}}{\partial \lambda_1}, \quad \bar{T}_{22} = \frac{\partial \tilde{W}}{\partial \lambda_2}, \quad (2.16)$$

and for the equilibrium configuration to be stable,  $\lambda_1$  and  $\lambda_2$  must satisfy the following inequalities:

$$\frac{\partial^2 \tilde{W}}{\partial \lambda_1^2} \geq 0, \quad \frac{\partial^2 \tilde{W}}{\partial \lambda_2^2} \geq 0, \quad \left( \frac{\partial^2 \tilde{W}}{\partial \lambda_1 \partial \lambda_2} \right)^2 \leq \frac{\partial^2 \tilde{W}}{\partial \lambda_1^2} \frac{\partial^2 \tilde{W}}{\partial \lambda_2^2}. \quad (2.17)$$

For equal normal dead loads on the edges,  $\bar{T}_{11} = \bar{T}_{22}$ . Thus

$$\frac{\partial \tilde{W}}{\partial \lambda_1} - \frac{\partial \tilde{W}}{\partial \lambda_2} = 0. \quad (2.18)$$

If both equal and unequal values of  $\lambda_1$  and  $\lambda_2$  satisfy (2.18), then there is a possibility of Treloar's instability occurring in the material with strain energy density given by  $W$ . In the  $\lambda_1\lambda_2$ -plane, let  $(\lambda_f, \lambda_f)$  be the point of intersection of the symmetric and the asymmetric solutions of (2.18). Since a membrane cannot support compressive edge loads, therefore  $\lambda_f$  must be greater than 1 for the occurrence of Treloar's instability. MacSithigh [5] has shown that the equilibrium equations and the boundary conditions are satisfied by negative stretches which correspond to the membrane undergoing two  $180^\circ$  rotations in the dead loading device. However, laboratory simulations of dead load tests do not permit such rotations, and will not be considered here.

### (ii) Inflation of a spherical balloon

We assume that a spherical balloon is deformed into a spherical balloon. With respect to the orthonormal set of coordinate axes aligned along the longitudinal, the latitudinal and the radial directions, the three principal stretches for the deformation gradient (2.1) are given by

$$\lambda_1 = \lambda_2 = \frac{r}{R}, \quad \lambda_3 = \frac{h}{H}, \quad (2.19)$$

where  $r$  and  $R$  are, respectively, the radial coordinates of a point in the deformed and the undeformed configurations. The thickness of the membrane in the deformed and the undeformed configurations is denoted by  $h$  and  $H$  respectively. The stress component  $\sigma_{33}$  is very small as compared to  $\sigma_{11}$  and  $\sigma_{22}$  and is usually neglected. Thus Equation (2.13)

determines  $\lambda_3$  as a function of  $\lambda_1$  and  $\lambda_2$ . The pressure difference,  $p$ , between the inside and the outside of the balloon is balanced by the membranal stresses  $\sigma_{11} = \sigma_{22}$ . Thus

$$p\pi r^2 = \sigma_{11}2\pi rh, \quad (2.20)$$

or equivalently

$$p = \frac{2H}{R} \frac{1}{\lambda_1^2} \frac{\partial \tilde{W}}{\partial \lambda_1}. \quad (2.21)$$

$p$  is usually called the pressure in the balloon since the atmospheric pressure on the outside of the balloon is negligible as compared to  $p$ .

In order to discuss the stability of the deformed configuration of a spherical balloon, we assume that it is connected to an infinite reservoir that supplies gas at a constant pressure  $p$  and at a constant temperature. In an equilibrium configuration, the potential

$$E(\lambda_1) = -p \left( \frac{4}{3} \pi R^3 \right) \lambda_1^3 + \hat{W}(\lambda_1), \quad (2.22)$$

should have the absolute or the relative minima [2]. Here  $-p(\frac{4}{3}\pi R^3) \lambda_1^3$  is a kind of potential energy associated with the work done by the gas on the balloon, and

$$\hat{W}(\lambda_1) = 4\pi R^2 H \tilde{W}(\lambda_1, \lambda_1). \quad (2.23)$$

Thus, in the equilibrium configuration,

$$p = \frac{1}{4\pi R^3 \lambda_1^2} \frac{\partial \hat{W}}{\partial \lambda_1}, \quad (2.24)$$

and for the equilibrium configuration to be stable

$$\frac{d^2 E}{d\lambda_1^2} = \frac{\partial^2 \hat{W}}{\partial \lambda_1^2} - \frac{2}{\lambda_1} \frac{\partial \hat{W}}{\partial \lambda_1} \geq 0, \quad (2.25)$$

or equivalently

$$\frac{dp}{d\lambda_1} \geq 0. \quad (2.26)$$

That is, the pressure,  $p$ , must be a non-decreasing function of the stretch  $\lambda_1$ .

### 3. ANALYSIS OF THE TWO PROBLEMS

#### 3.1. Biaxial Stretching of a Rectangular Membrane

##### 3.1.1. Harmonic Material

Substitution from (2.5) and (2.6) into (2.13) gives

$$\lambda_3 = (\lambda_1 \lambda_2 - 1)/2\alpha - (\lambda_1 + \lambda_2 - 3). \quad (3.1)$$

Since  $\lambda_3 > 0$ , therefore positive values of  $\lambda_1$  and  $\lambda_2$  must be such that

$$\lambda_1 \lambda_2 - 1 > 2\alpha (\lambda_1 + \lambda_2 - 3). \quad (3.2)$$

Equation (3.1) when combined with Equations (2.5) and (2.6) gives

$$\tilde{W} = \frac{\mu_0}{2\alpha} [-(\lambda_1 \lambda_2 - 1)^2 + 4\alpha \lambda_1 \lambda_2 (\lambda_1 + \lambda_2 - 3) + 4\alpha]. \quad (3.3)$$

Substitution from (3.3) into (2.16) yields

$$\begin{aligned} \bar{T}_{11} &= \frac{\mu_0}{\alpha} [\lambda_2 - \lambda_1 \lambda_2^2 + 4\alpha \lambda_1 \lambda_2 + 2\alpha \lambda_2^2 - 6\alpha \lambda_2], \\ \bar{T}_{22} &= \frac{\mu_0}{\alpha} [\lambda_1 - \lambda_2 \lambda_1^2 + 4\alpha \lambda_1 \lambda_2 + 2\alpha \lambda_1^2 - 6\alpha \lambda_1]. \end{aligned} \quad (3.4)$$

Thus

$$\bar{T}_{11} - \bar{T}_{22} = \frac{\mu_0}{\alpha} (\lambda_2 - \lambda_1) (1 + 2\alpha (\lambda_1 + \lambda_2 - 3) - \lambda_1 \lambda_2). \quad (3.5)$$

Because of (3.2), Equation (3.5) gives  $\lambda_1 = \lambda_2$  for  $\bar{T}_{11} = \bar{T}_{22}$ . Thus this material does not admit Treloar's instability. In order to see if the deformed equilibrium configuration is stable or not, we substitute for  $\tilde{W}$  from (3.3) into (2.17) and obtain

$$\lambda (4\alpha - \lambda) \geq 0, \quad (8\alpha \lambda + 1 - 6\alpha - 2\lambda^2)^2 \leq \lambda^2 (4\alpha - \lambda)^2, \quad (3.6)$$

where we have set  $\lambda_1 = \lambda_2 = \lambda$ . Recalling (3.2),  $\lambda$  must also satisfy

$$\lambda^2 - 1 > 2\alpha (2\lambda - 3). \quad (3.7)$$

Inequality (3.7) implies (3.6)<sub>2</sub>. For a given  $\nu_0$ , one can find the maximum value of  $\lambda$  satisfying the two inequalities (3.6)<sub>1</sub> and (3.7). For  $\lambda < 4\alpha$ , strict inequality holds in (3.6)<sub>1</sub>. However, (3.7) is violated for  $\lambda = 2\alpha \pm \sqrt{4\alpha^2 - 6\alpha + 1}$ . For example, for  $\alpha = 1.5$  which corresponds to  $\nu_0 = 0.4$ , (3.7) is violated for  $2 \leq \lambda \leq 4$ . Thus if equal dead normal edge loads on a rectangular membrane made of this material are gradually increased, then the maximum equal biaxial stretches that can be observed are 2. If  $0 < \nu_0 < 0.382$ , then  $4\alpha^2 < (6\alpha - 1)$  and inequalities (3.6)<sub>1</sub> and (3.7) are satisfied for  $\lambda < 5.236$ .

The nominal normal edge traction  $\bar{T}$  required to produce the stretch  $\lambda$  is given by

$$\bar{T} = \frac{\mu_0}{\alpha} (\lambda - 1) [(6\alpha - 1)\lambda - \lambda^2]. \quad (3.8)$$

The plot of  $\bar{T}$  vs  $\lambda$  depends strongly upon the value assigned to  $\nu_0$ . For  $\nu_0$  close to 0.25 the curve  $\bar{T}$  vs  $\lambda$  is concave downwards; the maximum value of  $\bar{T}$  occurs for the largest value of  $\lambda$  that satisfies inequalities (3.6) and (3.7). For  $\nu_0 > 0.3$ , the maximum value of  $\lambda$  that satisfies inequalities (3.6) and (3.7) and where  $\bar{T}$  attains a maximum value do not coincide with each other.

### 3.1.2. Generalized Blatz–Ko Material

Substitution from (2.8) into (2.13) gives

$$\lambda_3 = (\lambda_1 \lambda_2)^{q/(2-q)}, \quad (3.9)$$

and all finite values of  $\lambda_1$  and  $\lambda_2$  are admissible. Equations (3.9), (2.16) and (2.8) give

$$\begin{aligned} \frac{2}{\mu_0} \tilde{W} = f & \left[ \left( \lambda_1^2 + \lambda_2^2 + (\lambda_1 \lambda_2)^{\frac{2q}{2-q}} - 3 \right) - \frac{2}{q} \left( (\lambda_1 \lambda_2)^{\frac{2q}{2-q}} - 1 \right) \right] \\ & + (1-f) \left[ \frac{1}{\lambda_1^2} + \frac{1}{\lambda_2^2} + (\lambda_1 \lambda_2)^{-\frac{2q}{2-q}} - 3 - \frac{2}{q} \left( (\lambda_1 \lambda_2)^{-\frac{2q}{2-q}} - 1 \right) \right], \quad (3.10) \end{aligned}$$

$$\frac{\bar{T}_{11}}{\mu_0} = f \left[ \lambda_1 - \lambda_2 (\lambda_1 \lambda_2)^{\frac{3q-2}{2-q}} \right] + (1-f) \left[ -\frac{1}{\lambda_1^3} + \lambda_2 (\lambda_1 \lambda_2)^{\frac{q+2}{q-2}} \right], \quad (3.11)$$

$$\frac{\bar{T}_{22}}{\mu_0} = f \left[ \lambda_2 - \lambda_1 (\lambda_1 \lambda_2)^{\frac{3q-2}{2-q}} \right] + (1-f) \left[ -\frac{1}{\lambda_2^3} + \lambda_1 (\lambda_1 \lambda_2)^{\frac{q+2}{q-2}} \right]. \quad (3.12)$$

The equality of normal dead loads on the edges (i.e.  $\bar{T}_{11} = \bar{T}_{22}$ ) gives the following: either  $\lambda_1 = \lambda_2$  or

$$f \left( 1 + (\lambda_1 \lambda_2)^{\frac{3q-2}{2-q}} \right) + (1-f) \left( \frac{\lambda_1^2 + \lambda_2^2 + \lambda_1 \lambda_2}{\lambda_1^3 \lambda_2^3} - (\lambda_1 \lambda_2)^{\frac{q+2}{q-2}} \right) = 0. \quad (3.13)$$

Note that

$$\frac{3q-2}{2-q} = -\frac{1+\nu_0}{1-\nu_0}, \quad \frac{q+2}{q-2} = -\frac{1-3\nu_0}{1-\nu_0}. \quad (3.14)$$

For  $f = 1$ , Equation (3.13) cannot be satisfied by positive values of  $\lambda_1$  and  $\lambda_2$ . Thus normal equal dead loads at the edges result in equal biaxial stretches.

For  $f = 0$ , the unequal roots of the equation  $\bar{T}_{11} = \bar{T}_{22}$  satisfy

$$\lambda_1^2 + \lambda_2^2 + \lambda_1 \lambda_2 - (\lambda_1 \lambda_2)^{\frac{2}{1-\nu_0}} = 0. \quad (3.15)$$

The point  $(\lambda_f, \lambda_f)$  in the  $\lambda_1 \lambda_2$ -plane where the symmetric and the asymmetric solutions intersect is given by

$$\lambda_f = \left( \frac{1}{3} \right)^{\frac{2(1+\nu_0)}{(1-\nu_0)}}. \quad (3.16)$$

For  $0 < \nu_0 < 0.5$ ,  $\lambda_f < 1$ . Thus Treloar's instability will not occur in the generalized Blatz–Ko material with  $f = 0$ .

For  $0 < f < 1$  and  $0 < \nu_0 < 0.5$ , the second term in (3.13) will become negative for large values of  $\lambda_1$  and  $\lambda_2$  and (3.13) is satisfied by positive values of  $\lambda_1$  and  $\lambda_2$ , and  $\lambda_f$  is given by



Table 1. Roots of Equation (3.17) for different values of  $\nu_0$  and  $f$ .

$f$	$\nu_0$		
	0.25	0.30	0.40
0.1	1.4775	—	1.301
0.2	1.6324	1.505	1.348
0.3	2.167	1.686	1.415
0.4	—	2.447	1.520
0.5	—	—	1.712

$$f \left( 1 + \lambda_f^{-\frac{2(1+\nu_0)}{1-\nu_0}} \right) + (1-f) \left( 3\lambda_f^{-4} - \lambda_f^{-\frac{2(1-3\nu_0)}{(1-\nu_0)}} \right) = 0. \quad (3.17)$$

We now have a two-parameter family of possible unequal principal stretches for equal biaxial loads. Out of the symmetric and the asymmetric solutions, the one that satisfies strict inequalities in (2.17) can be observed experimentally. Substitution from (3.10) into (2.17) gives

$$g_1 \equiv f \left[ 1 - \frac{3q-2}{2-q} \lambda_2^2 (\lambda_1 \lambda_2)^{\frac{4(q-1)}{2-q}} \right] + (1-f) \left[ \frac{3}{\lambda_1^4} + \frac{q+2}{q-2} \lambda_2^2 (\lambda_1 \lambda_2)^{\frac{4}{q-2}} \right] \geq 0, \quad (3.18_1)$$

$$g_2 \equiv f \left[ 1 - \frac{3q-2}{2-q} \lambda_1^2 (\lambda_1 \lambda_2)^{\frac{4(q-1)}{2-q}} \right] + (1-f) \left[ \frac{3}{\lambda_2^4} + \frac{q+2}{q-2} \lambda_1^2 (\lambda_1 \lambda_2)^{\frac{4}{q-2}} \right] \geq 0, \quad (3.18_2)$$

$$G \equiv g_1 g_2 - \left( \frac{2q}{2-q} \right)^2 \left[ f (\lambda_1 \lambda_2)^{\frac{3q-2}{2-q}} + (1-f) (\lambda_1 \lambda_2)^{\frac{q+2}{q-2}} \right]^2 \geq 0. \quad (3.18_3)$$

For  $\nu_0 = 0.25, 0.3$  and  $0.4$ , and starting from  $f = 0.1$ ,  $f$  was incremented by  $0.1$  until Equation (3.17) ceased to have roots greater than  $1.0$ ; results are summarized in Table 1.

For  $f = 0.3$  and  $\nu_0 = 0.3$ , Figure 1 depicts values of  $\lambda_1$  and  $\lambda_2$  that satisfy (3.13) and also the line  $\lambda_1 = \lambda_2$ . The two curves intersect at the point  $(1.686, 1.686)$ . Both equal and unequal roots of (3.13) satisfy strict inequalities (3.18)<sub>1-3</sub> and thus correspond to stable solutions. The tractions for the symmetric solution increase monotonically with the stretch while that for the asymmetric solution monotonically decrease; see Figure 2. Thus in the laboratory, the membrane will begin deforming symmetrically till  $\lambda_1 = \lambda_2 = \lambda_f$ . For a further increase in the tractions both symmetric and the asymmetric solutions are possible. Since the free enthalpy of the asymmetric solution is less than that of the symmetric solution for  $\lambda_1 = \lambda_2 > \lambda_f$ , the deformations will suddenly switch from the symmetric to the asymmetric pattern.

For the Mooney–Rivlin material the symmetric solution is unstable for  $\lambda_1 = \lambda_2 > \lambda_f$ .

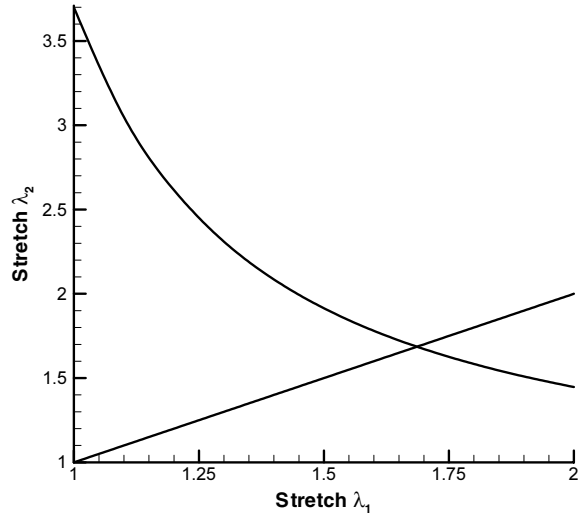


Figure 1. Asymmetric (—) and symmetric (- -) solutions for principal stretches in a biaxially loaded rectangular Blatz–Ko membrane with equal nominal surface tractions.

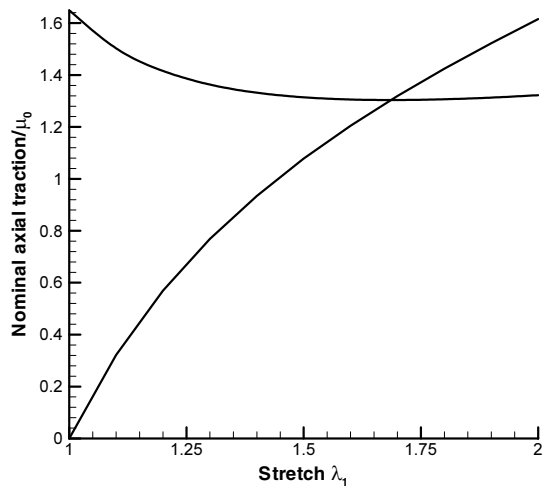


Figure 2. Normalized nominal axial traction rs.  $\lambda_1$  for a biaxially loaded rectangular Blatz–Ko membrane with equal nominal surface tractions; — unequal biaxial stretches, - - - equal biaxial stretches.

### 3.1.3. *St Venant–Kirchhoff Material*

Recalling that

$$II_E = \frac{1}{2}[I_E^2 - \text{tr}(\mathbf{E}^2)], \quad (3.19)$$

Equation (2.11) becomes

$$W = \frac{\lambda_0}{8}(\lambda_1^2 + \lambda_2^2 + \lambda_3^2 - 3)^2 + \frac{\mu_0}{4}[(\lambda_1^2 - 1)^2 + (\lambda_2^2 - 1)^2 + (\lambda_3^2 - 1)^2]. \quad (3.20)$$

Substitution from (3.20) into (2.13) yields

$$\lambda_3^2 = \frac{3\lambda_0 + 2\mu_0 - \lambda_0(\lambda_1^2 + \lambda_2^2)}{\lambda_0 + 2\mu_0}, \quad (3.21)$$

where we have assumed that  $\lambda_0 + 2\mu_0 > 0$ . Since  $\lambda_3^2 > 0$ , therefore

$$\lambda_1^2 + \lambda_2^2 < 3 + 2\frac{\mu_0}{\lambda_0} = 1 + 1/\nu_0. \quad (3.22)$$

Thus a material with a small positive value of  $\nu_0$  can possibly sustain large values of  $\lambda_1$  and  $\lambda_2$ . Equations (3.20) and (3.21) give the following expression for the strain energy density per unit reference volume as a function of  $\lambda_1$  and  $\lambda_2$ :

$$\frac{\tilde{W}}{\mu_0}(\lambda_1, \lambda_2) = \frac{\beta_0}{4}(\lambda_1^2 + \lambda_2^2 - 2)^2 + \frac{1}{4}[(\lambda_1^2 - 1)^2 + (\lambda_2^2 - 1)^2], \quad (3.23)$$

where

$$\beta_0 = \frac{\lambda_0}{\lambda_0 + 2\mu_0} = \frac{\nu_0}{1 - \nu_0}. \quad (3.24)$$

Equations (2.16) and (3.23) give

$$\frac{\bar{T}_{11}}{\mu_0} = \beta_0\lambda_1(\lambda_1^2 + \lambda_2^2 - 2) + \lambda_1(\lambda_1^2 - 1), \quad (3.25)$$

$$\frac{\bar{T}_{22}}{\mu_0} = \beta_0\lambda_2(\lambda_1^2 + \lambda_2^2 - 2) + \lambda_2(\lambda_2^2 - 1). \quad (3.26)$$

Thus  $\bar{T}_{11} = \bar{T}_{22}$  holds when either  $\lambda_1 = \lambda_2$  or

$$\lambda_2 = \frac{-\lambda_1 + [4 - 3\lambda_1^2 + 4\beta_0(3 - 2\lambda_1^2) + 4\beta_0^2(2 - \lambda_1^2)]^{1/2}}{2(1 + 2\beta_0)}. \quad (3.27)$$

Equation (3.27) could have also been deduced from Equation (12a) of [18]. The point  $(\lambda_f, \lambda_f)$  in the  $\lambda_1\lambda_2$ -plane where the symmetric and the asymmetric solutions intersect is given by

$$\lambda_f^2 = \frac{1 + 2\beta_0}{3 + 2\beta_0} = \frac{1 + \nu_0}{3 - \nu_0}. \quad (3.28)$$

For  $0 < \nu_0 < 0.5$ ,  $\lambda_f < 1$ .

The stability conditions (2.17) become

$$\begin{aligned} \beta_0(3\lambda_1^2 + \lambda_2^2) + 3\lambda_1^2 - (1 + 2\beta_0) &\geq 0, \\ \beta_0(\lambda_1^2 + 3\lambda_2^2) + 3\lambda_2^2 - (1 + 2\beta_0) &\geq 0, \\ [\beta_0(3\lambda_1^2 + \lambda_2^2) + 3\lambda_1^2 - (1 + 2\beta_0)][\beta_0(\lambda_1^2 + 3\lambda_2^2) \\ + 3\lambda_2^2 - (1 + 2\beta_0)] - 4\beta_0^2\lambda_1^2\lambda_2^2 &\geq 0. \end{aligned} \quad (3.29)$$

When  $\lambda_1 = \lambda_2 = \lambda$ , the satisfaction of (3.29)<sub>3</sub> implies that conditions (3.29)<sub>1</sub> and (3.29)<sub>2</sub> are satisfied. Furthermore, (3.22) and (3.29)<sub>3</sub> require that

$$\frac{1 + \nu_0}{2\nu_0} > \lambda^2 \geq \frac{1 + 2\beta_0}{3 + 2\beta_0} = \frac{1 + \nu_0}{3 - \nu_0}. \quad (3.30)$$

From (3.28) and (3.30) we conclude that equal normal dead loads on the edges of a rectangular membrane made of the St Venant–Kirchhoff material produce equal principal stretches in the directions of the dead loads. Thus Treloar's instability can not occur in a rectangular membrane made of the St Venant–Kirchhoff material.

### 3.2. Inflation of a Spherical Balloon

#### 3.2.1. Harmonic Material

Substitution from (3.3) into (2.21) and setting  $\lambda_2 = \lambda_1 = r/R$  gives

$$\bar{p} \equiv \frac{\alpha R}{2\mu_0 H} p = 6\alpha - (6\alpha - 1)\frac{R}{r} - \frac{r}{R}, \quad (3.31)$$

for the non-dimensional pressure,  $\bar{p}$ , as a function of the present radius  $r$ . It follows from Equation (3.2) that Equation (3.31) holds so long as

$$r^2 - 4\alpha rR + (6\alpha - 1)R^2 > 0. \quad (3.32)$$

The pressure,  $\bar{p}$ , becomes maximum at  $r = r_{\max} = R\sqrt{(6\alpha - 1)}$ , and deformations become unstable for  $r > r_{\max}$ . For  $\nu_0 = 0.25$ ,  $r_{\max} = \sqrt{3.5}R$ . Since  $d\bar{p}/dr = 0$  has only one root,  $r = r_{\max}$ , and  $d^2\bar{p}/dr^2|_{r=r_{\max}} < 0$ , therefore the pressure vs the present radius curve is monotonically increasing until  $r = r_{\max}$  and monotonically decreasing for  $r > r_{\max}$ .

#### 3.2.2. Generalized Blatz–Ko Material

From (2.19), (2.21) and (3.10) we obtain the following expression for the non-dimensional pressure,  $\bar{p}$ , in a spherical balloon made of a generalized Blatz–Ko material:

$$\tilde{p} = \frac{p}{\mu_0} \frac{R}{H} = f \left( \frac{R}{r} - \left( \frac{r}{R} \right)^{\frac{7q-6}{2-q}} \right) + (1-f) \left( -\frac{R^5}{r^5} + \left( \frac{r}{R} \right)^{\frac{q+6}{q-2}} \right). \quad (3.33)$$

Equation (3.9) relates, in the current configuration, the thickness of the balloon to its radius

$$\frac{h}{H} = \left( \frac{r}{R} \right)^{\frac{2q}{2-q}}. \quad (3.34)$$

The deformed configuration of the balloon will be stable or metastable according as inequality or equality holds in the following:

$$-f \left( \frac{R^2}{r^2} + \frac{7q-6}{2-q} \left( \frac{r}{R} \right)^{\frac{8q-8}{2-q}} \right) + (1-f) \left( 5 \left( \frac{R}{r} \right)^6 + \frac{q+6}{q-2} \left( \frac{r}{R} \right)^{\frac{8}{q-2}} \right) \geq 0. \quad (3.35)$$

Note that

$$\frac{7q-6}{2-q} = -\frac{(3+\nu_0)}{(1-\nu_0)}, \quad \frac{q+6}{q-2} = \frac{(7\nu_0-3)}{(1-\nu_0)}.$$

For  $f = 0$  and  $3/7 \leq \nu_0 < 0.5$ , the deformed shape of the balloon is always stable. For  $0 < \nu_0 < 3/7$ , only those shapes for which  $r < R \left( \frac{1}{5} \frac{3-7\nu_0}{1-\nu_0} \right)^{\frac{q-2}{4-6q}}$  are stable. For  $f = 0$  and  $q = -1$  Haughton [8] found that the maximum in the pressure occurs at  $r/R = 1.39$ , which agrees with our result.

For  $f = 1$ , stable configurations of the balloon are given by

$$r < R \left[ \frac{3+\nu_0}{1-\nu_0} \right]^{\frac{2-q}{4-6q}}.$$

For  $\nu_0 = 0.3$  and  $f = 0, 0.3$  and  $1.0$ , plots of  $\tilde{p}$  vs  $r/R$  show that the pressure increases monotonically until  $r/R \simeq 1.441, 1.463$  and  $1.518$  respectively. For stretches exceeding these values,  $d\tilde{p}/dr < 0$  and the deformed shape of the balloon will be unstable.

### 3.2.3. *St Venant–Kirchhoff Material*

Equations (2.21) and (3.23) yield the following relation between the non-dimensional pressure,  $\hat{p}$ , as a function of the present radius  $r$ :

$$\hat{p} \equiv \frac{p}{\mu_0} \frac{R}{2H} = (1 + 2\beta_0) \left( \frac{r}{R} - \frac{R}{r} \right). \quad (3.36)$$

Equation (3.22) implies that

$$r < R(0.5 + 0.5/\nu_0)^{1/2}. \quad (3.37)$$

It follows from Equation (3.36) that the pressure is a monotonically increasing function of the radius  $r$ . Hence deformations of the spherical balloon stay stable until the maximum radius  $r_{\max} = R(0.5 + 0.5/\nu_0)^{1/2}$  is reached. The maximum attainable radius is limited by the Poisson ratio for infinitesimal deformations.

#### 4. CONCLUDING REMARKS

For in-plane homogeneous deformations of a homogeneous membrane made of an incompressible material, the stretch in the transverse direction is determined by the requirement that deformations be isochoric. Thus, the transverse stretch does not become zero for finite values of in-plane stretches. However, for a compressible material, the requirement that the transverse stretch be positive may limit values of in-plane principal stretches. Material moduli limit in-plane principal stretches for the harmonic and the St Venant–Kirchhoff materials but not for the generalized Blatz–Ko material.

Of the three compressible hyperelastic materials studied herein, only the generalized Blatz–Ko material for some suitable values of material parameters exhibits Treloar’s instability associated with the occurrence of unequal principal stretches in biaxial loading of a uniform homogeneous square membrane with equal nominal tensile tractions (dead loads) at the edges. During the uniform inflation of a spherical balloon, the pressure–radius relation for each of the three materials does not have two branches on which the pressure increases monotonically with the radius. We note that a Mooney–Rivlin material but not a neo-Hookean material, both of which are incompressible, admits Treloar’s instability and a non-monotonic pressure–radius relationship for a spherical balloon. Kearsley [1] has shown that an isotropic incompressible hyperelastic material with  $(\partial W/\partial I_1)/(\partial W/\partial I_2) > 0$  admits Treloar’s instability.

It should be noted that only a limited class of homogeneous deformations has been considered while analyzing the stability of a deformed configuration of either a rectangular membrane or a spherical balloon. It is possible that the analysis of the stability of the deformed configuration under all admissible deformations will yield different results.

*Acknowledgements.* This work was partially supported by the Alexander von Humboldt Award.

#### REFERENCES

- [1] Kearsley, E. A. Asymmetric stretching of a symmetrically loaded elastic sheet. *International Journal of Solids and Structures*, 22, 111–119 (1986).
- [2] Ericksen, J. L. *Introduction to Thermodynamics of Solids*, Chapman and Hall, London, 1991.
- [3] Chen, Y. C. Stability of homogeneous deformations of an incompressible elastic body under dead-load surface tractions. *Journal of Elasticity*, 77, 223–248 (1987).
- [4] Müller, I. Two instructive instabilities in non-linear elasticity: biaxially loaded membrane, and rubber balloons. *Mechanica*, 31, 387–395 (1976).
- [5] MacSithigh, G. P. Energy-minimal finite deformations for a symmetrically loaded elastic sheet. *Quarterly Journal of Mechanics and Applied Mathematics*, 39, 111–123 (1986).
- [6] Alexander, H. Tensile instability of initially spherical balloons. *International Journal of Engineering Science*, 9, 151–162 (1971).
- [7] Chen, Y.-C. and Healey, T. J. Bifurcation to pear-shaped equilibria of pressurized spherical membranes. *International Journal of Non-Linear Mechanics*, 26, 279–291 (1991).
- [8] Haughton, D. M. Inflation and bifurcation of compressible spherical membranes. *Journal of Elasticity*, 12, 239–245 (1982).
- [9] Carroll, M. M. Pressure maximum behavior in inflation of incompressible elastic hollow spheres and cylinders. *Quarterly of Applied Mathematics*, 45, 141–154 (1987).
- [10] Ogden, R. W. Large deformation isotropic elasticity: on the correlation of theory and experiments for compressible rubberlike solids. *Proceedings of the Royal Society of London A*, 328, 567–577 (1972).
- [11] Rivlin, R. S. Stability of pure homogeneous deformations of an elastic cube under dead loading. *Quarterly of Applied Mathematics*, 32, 265–272 (1974).

- [12] John, F. Plane strain problems for a perfectly elastic material of harmonic type. *Communications in Pure and Applied Mathematics*, 13, 239–296 (1960).
- [13] John, F. Plane elastic waves of finite amplitude. Hadamard materials and harmonic materials. *Communications in Pure and Applied Mathematics*, 19, 309–341 (1966).
- [14] Blatz, P. J. and Ko, W. L. Application of finite elastic theory to the deformation of rubbery materials. *Transactions of the Society of Rheology*, 6, 223–251 (1962).
- [15] Beatty, M. F. Topics in finite elasticity: hyperelasticity of rubber, elastomers, and biological tissues—with examples. *Applied Mechanics Reviews*, 40, 1699–1734 (1987).
- [16] Truesdell, C. A. and Noll, W. *The Non-Linear Field Theories of Mechanics*, Handbuch der Physik, ed. S. Flügge, Springer, Berlin, 1965.
- [17] Treloar, L. R. G. Stresses and birefringence in rubber subjected to general homogeneous strain. *Proceedings of the Physical Society*, 60, 135–144 (1948).
- [18] Batra, R. C. Comparison of results from four linear constitutive relations in isotropic finite elasticity. *International Journal of Nonlinear Mechanics*, 36, 421–432 (2001).
- [19] Ogden, R. W. and Isherwood, D. A. Solutions of some finite plane strain problems for compressible elastic solids. *Quarterly Journal of Mechanics and Applied Mathematics*, 31, 219–249 (1978).
- [20] Abeyaratne, R. and Horgan, C. O. The pressurized hollow sphere problem in finite elastostatics for a class of compressible materials. *International Journal of Solids and Structures*, 20, 715–725 (1984).
- [21] Jafari, A. H., Abeyaratne, R. and Horgan, C. O. The finite deformation of a pressurized circular tube for a class of compressible materials. *Zeitschrift für Angewandte Mathematik und Physik*, 35, 227–246 (1984).
- [22] Knowles, J. K. and Sternberg, E. On the singularity induced by certain mixed boundary conditions in linearized and nonlinear elastostatics. *International Journal of Solids and Structures*, 11, 1173–1201 (1975).
- [23] Haughton, D. M. and Lindsay, K. A. The second-order deformation of a finite compressible isotropic elastic annulus subjected to circular shearing. *Proceedings of the Royal Society of London A*, 442, 621–639 (1993).